Bull Volcanol (1999) 61:106–120

ORIGINAL PAPER

W. I. Rose · F. M. Conway · C. R. Pullinger
A. Deino · W. C. McIntosh

An improved age framework for late Quaternary silicic eruptions in northern Central America

Received: 15 May 1998 / Accepted: 18 January 1999

Abstract Five new stepwise-heating $^{40}Ar/^{39}Ar$ ages and one new high-sensitivity ^{14}C date of ash-fall and ash-flow deposits from late Quaternary silicic volcanoes in northern Central America document the eruption rates and frequencies of five major rhyodacite and rhyolite calderas (Atitlán, Amatitlán, Ayarza, Coatepeque, and Ilopango) located north of the basalt, andesite, and dacite stratovolcanoes of the Central American volcanic front. These deposits form extensive time-stratigraphic horizons that intercalate regionally, and knowledge of dates and stratigraphy provides a valuable framework for age determinations of more localized volcanic and nonvolcanic events. The new data, especially when integrated with previous stratigraphic and dating work, show that all five calderas erupted several times in the past 200 ka and, despite a lack of historic activity, should be considered as active centers that could produce highly explosive eruptions again. Because of their locations near the highly vulnerable economic hearts of Guatemala and El Salvador, the risks of eruptions from these calderas should be carefully considered along with risks of major earthquakes and volcanic front volcanoes, which are much more frequent but inflict less severe and extensive damage. This investigation also includes some examples of dating efforts that failed to produce reasonable results.

Key words Ages · Calderas · Late Quaternary · Guatemala · El Salvador

Editorial responsibility: S. Carey

William I. Rose (✉) · Carlos Pullinger
Geological Engineering and Sciences, Michigan Technological University, Houghton, MI 49931 USA
e-mail: raman@mtu.edu pulga@salnet.net

F. Michael Conway
Division of Science and Math, Arizona Western College, Box 929, Yuma, AZ 85366, USA

Alan Deino
Berkeley Geochronology Center, 2455 Ridge Rd., Berkeley, CA 94709, USA

William C. McIntosh
New Mexico Geochronology Research Laboratory, N.M. Bureau of Mines, New Mexico Tech, 801 Leroy Place, Socorro, New Mexico, 87801–4796, USA

Introduction

Silicic volcanism is prominent in northern Central America. Major centers are marked by a chain of caldera lakes (Atitlán, Amatitlán, Ayarza, Coatepeque, and Ilopango) a few kilometers north of the volcanic front (Fig. 1). A stratigraphic framework for these silicic centers exists, but reliable radiometric ages are either too few or too imprecise to define their history very clearly. The silicic deposits of these calderas provide a complex stratigraphic record that intercalates between adjacent silicic centers and late Quaternary arc-front composite volcanoes (Fig. 2; Koch and McLean 1975;

Fig. 1 Location map showing late Quaternary calderas of northern Central America

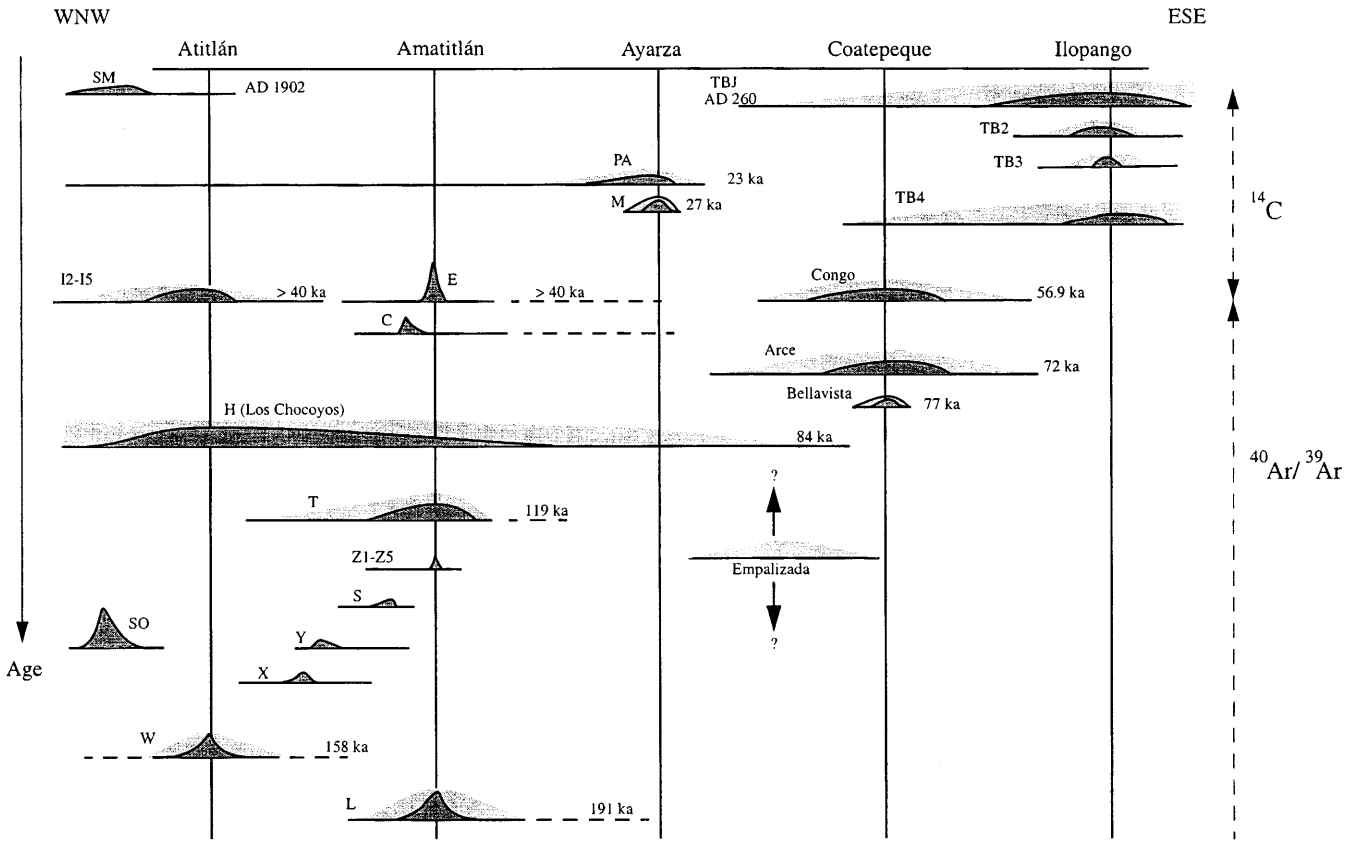

Fig. 2 Schematic composite cross-section diagram fromWNWto ESE, showing the stratigraphic relationships and dates of late Quaternary tephra units discussed in this paper. Approximate extent of the deposits is shown by the *solid line* and the extent of pyroclastic flow deposits by the *light stipple pattern*. The units and their dates are from Table 1

Rose et al. 1980; Carr et al. 1981). Except for their spatial positions, the relationships (i.e., shared plumbing systems) between the silicic volcanic centers and the volcanic front are not well known. Historical activity is common from the front but unknown from these calderas, so the risk of eruptions from the calderas is not quantified. The volume of eruptive material from silicic volcanoes over the past 200 ka is approximately equivalent to the volume of eruptive materials from the volcanic front (Rose et al. 1981), but much activity of the volcanic front appears to be younger than the most voluminous silicic eruptions.

We present five new, stepwise-heating $^{40}Ar/^{39}Ar$ ages and one new ^{14}C age of ash-fall and ash-flow deposits, including three new ages from the largest and most long-lived of the Quaternary silicic centers, Atitlán and Amatitlán calderas, and three new ages from Coatepeque caldera. The ages constrain the timing of major events and by inference the lengths of intervening reposes at the three calderas. Because of pervasive interfingering of tephra, the new dates provide a regional age framework for middle to late Quaternary silicic activity of northern Central America. In addition, inferences can be made about long-term volcanic hazards in the same region, particularly the risk of eruptions from silicic centers, less frequent but devastating when they do occur. Because these calderas are all marked by picturesque lakes and have geothermal potential, they are focal points for development in Guatemala and El Salvador and are places where risk assessment is a priority.

Volcanic setting

The Central American volcanic arc stretches 1100 km from the Guatemalan–Mexico border to northern Panama (Carr and Stoiber 1990). Cenozoic calc-alkalic volcanic activity in northern Central America has persisted since at least the Eocene (Donnelly et al. 1990). Wadge (1984) estimated that the current rate of production of volcanic products for the Central American arc is 31–62 km^3/Ma for each kilometer of arc. In northern Central America, the mid- to late Quaternary volcanic arc comprises 12 large composite volcanoes and several dacite domes (Meyer-Abich 1956); five major silicic centers are situated behind the arc (Fig. 1). Ash-flow deposits of the five calderas cover broad areas in both Guatemala (Hahn et al. 1979) and El Salvador (Hart 1983). The combined total volume of ash-flow and ash-fall deposits less than approximately 200 ka is conservatively estimated between 300 and 500 km^3 (Rose et al. 1981), similar to the volume of andesitic

and basaltic material erupted from the youngest generation of volcanic front volcanoes. Activity at silicic calderas largely antedates but partly overlaps activity of the present generation of ~50 ka and younger composite volcanoes (Koch and McLean 1975; Rose et al. 1981; Conway et al. 1994).

A framework for the Quaternary tephrostratigraphy and tephrochronology of the Guatemalan Highlands was laid out in a landmark paper by Koch and McLean (1975). The authors documented the mineralogy, geochemistry, distribution, and potential source vents of major tephra deposits. Building on this work, Rose and co-workers (1981) constructed isopach maps of major tephra units. This allowed for accurate volume estimates of tephra units and resolved questions about source vents (Rose et al. 1981; Drexler 1979; Hahn et al. 1979; Wunderman and Rose 1984; Rose et al. 1987; Peterson and Rose 1985). Deposits of young (<200 ka) silicic centers in northern Central America comprise numerous fall deposits and at least ten pyroclastic flow deposits (Koch and McLean 1975; Rose et al. 1981).

Koch and McLean (1975) recognized two stratigraphic successions in the Volcanic Highlands. An upland succession, confined to ridges and valley walls, comprises intercalated fall units and paleosols. A basin succession, which infills intermontane basins to depths as great as 200 m, consists of fall deposits and valley-fill pyroclastic flow deposits intercalated with paleosols. Locally, the valley-fill succession rests on discontinuous fluvial deposits and paleosols, and on reversely magnetized (Matuyama, >0.78 Ma; Cande and Kent 1995) andesite lava flows (Wunderman and Rose 1984) that overlie a loosely correlated series of ash-fall and ash-flow tuffs designated the R-tephra (Koch and McLean 1975). Because dating of the deposits that overlie the reversed rocks has yielded ages that are all <200 ka, we do not consider that the R tephra, which must be at least 0.5 million years older, is part of the modern caldera record. The L fall and pyroclastic flow rest conformably on the reversed sequence. L is the oldest Bruhnes (<0.78 Ma) silicic tephra deposit of Guatemala and thus marks the onset of activity at the present generation of calderas.

Atitlán caldera

Williams' (1960) reconnaissance of the Atitlán caldera (Fig. 1) initiated caldera studies in Central America. Newhall's (1980, 1987) work demonstrated that caldera formation at Atitlán was episodic and that three distinct caldera formation events had occurred there over the past 12 Ma. The youngest caldera-associated deposits consist of units called W fall and flow, the Los Chocoyos Ash (consisting of the H fall and an ash-flow deposit), and a group of partly phreatomagmatic falls called I-fall deposits (Fig. 2). The details and compositional data on the deposits of the younger caldera are summarized by Rose et al. (1987). The Los Chocoyos Ash has attracted the most attention, because of its large volume [>200 km^3 dense rock equivalent (DRE), the largest unit known in the Guatemalan Quaternary sequence], its extent as nonwelded valley-fill deposits scattered across the Guatemalan Highlands (Hahn et al. 1979), and the occurrance of fall deposits in three ocean basins extending from the Gulf of Mexico near Florida to the Equatorial Pacific near Ecuador (Drexler et al. 1980). The Los Chocoyos Ash is the product of the latest sequence of caldera-forming eruptions at Atitlán and has been dated from oxygen-isotope anomalies in ocean-sediment cores, where the H fall is 84±5 ka (Drexler et al. 1980). Halsor (1989), Penfield et al. (1986), and Halsor and Rose (1988, 1991) investigated the plumbing system and petrogenesis of late-Quaternary to Holocene composite volcanoes bordering the Atitlán caldera (San Pedro, Atitlán, and Tolimán).

Amatitlán caldera

Deposits of the 16-km-long Amatitlán caldera (Fig. 1) were first studied by Eggers (1972) and Koch and McLean (1975). The caldera was recognized and defined by Wunderman and Rose (1984), who improved on the volcanic stratigraphy of Eggers (1972), and determined that nine pyroclastic units, with a combined total volume of 60–80 km^3 DRE, had erupted from the caldera. The principal units are the L fall and flow, the Z1–Z5 fall deposits, the T fall and flow, and the E-fall deposit (Fig. 2). The largest events were the L and T, which produced major pyroclastic flow sheets associated with caldera collapse.

Ayarza caldera

The eruptive history of the compound Ayarza caldera was reported by Petersen and Rose (1985). Initial explosive activity produced the Mixta fall and flow deposits (M in Fig. 2) with spectacular basalt–rhyolite mixed character and formed the eastern side of the compound caldera. A second eruption produced the much more extensive Piños Altos (PA) fall deposit and the phreatomagmatic Tapalapa flow. Carbon-14 ages of 27±1.6 ka from charcoal in the Mixta ashflow and 23±0.5 ka from charcoal in the Tapalapa flow deposit show that the two Ayarza eruptive events were only a few thousand years apart. The volumes of erupted material (~2 km^3 DRE) and the size of the caldera (3×5 km) are much smaller than the others discussed herein.

Coatepeque caldera

The Coatepeque caldera is a 6.5×11.5-km collapse caldera elongated northeastward and located approxi-

mately 50 km west of San Salvador. Inside, a lake by the same name measures 5 × km and has a total depth of approximately 120 m (Williams and Meyer-Abich 1955). The caldera walls rise from 250 m above the lake level (elevation 750 m) on the northeast rim to 950 m on the southwest rim. It is the second largest of the young generation of collapse calderas in El Salvador (after Ilopango caldera) and has produced approximately 24 km^3 DRE (CEL 1992a) of pyroclastic material that reaches the border with Guatemala and partially covers southwestern El Salvador.

Deposits associated with three major and one minor eruption are, from oldest to youngest, Bellavista, Arce, perlitic (minor), Congo deposits (Pullinger 1998). The ignimbrite sheets associated with these deposits extend up to 10–15 km away from the caldera in south, east, and north directions. To the west the sheets are covered by younger deposits from the Santa Ana volcanic complex. Tephra fallout deposits interfinger with Ilopango tephras close to San Salvador and overlie the H fall from Atitlán caldera in western El Salvador (Fig. 2). The Empalizada fall deposit (Fig. 2) originates from the "Concepción de Ataco" caldera, approximately 100 km west of San Salvador. This deposit has been found underlying both Atitlán's H-fall and Coatepeque's Arce-fall deposits.

Williams and Meyer-Abich (1955), in their "account of a hurried reconnaissance," offer a thorough description of the tephra deposits and suggest that the caldera was formed by the "engulfment of the old cones into the reservoirs below as a result of gravitative settling along ring fractures." Meyer (1964), based on heavy mineral distribution, reconstructed the tephrostratigraphy of the caldera. More recently, the national power company "Comisión Ejecutiva Hidroeléctrica del Rio Lempa" (CEL 1992a), during its geothermal exploration projects in the area, refined the stratigraphy and collected abundant rock samples for geochemical and petrographic analysis and for radiometric dating. They reported a $K/^{40}Ar$ age of 70 ± 2 ka on sanidine from the Arce tephras and, based on the limits of the ^{14}C method, a date of more than 40 ka for the overlying Congo tephras. The westernmost part of El Salvador has been explored extensively for geothermal resources by CEL, and as a result abundant information exists. CEL (1992a, b), among abundant ignimbrite deposits in this area, identified the Empalizada tephra, which underlies all Coatepeque tephras, and proposed a date of 0.35 Ma based on stratigraphic constraints.

Ilopango caldera

Ilopango caldera is an 8 × 11-km depression elongated eastward and filled by a lake of the same name in the eastern outskirts of the capital city, San Salvador (population ~2 million). Its named deposits, from youngest to oldest, are Tierra Blanca Joven (TBJ) and TB2-TB4. These deposits are related to at least four major eruptions and are found up to 20 km to the east, north, and south, where they control the topography, and as far away as 80 km to the west, where up to 0.3 m of the most recent airfall tephra have been found. Central El Salvador, particularly around the capital city, is marked by a young sequence of andesitic to rhyolitic air-fall and pyroclastic flows from San Salvador Volcano and Ilopango caldera, separated by poorly to well-developed paleosols. This sequence overlies andesitic to basaltic lava flows and related deposits from the ancestral San Salvador Volcano and Pliocene volcanic centers along the Balsamo range, south of the capital city. Studies of Ilopango caldera began with Williams and Meyer-Abich (1955) who noticed that the various episodes of large eruptions were followed by caldera collapse. Recently, more attention has been given to the youngest Ilopango unit, the phreatomagmatic TBJ tephra. Sheets (1983) reported a composite radiocarbon age of AD 260 ± 114 from carbonized logs in pyroclastic flow deposits. Hart (1981, 1983) studied the TBJ in detail, described numerous stratigraphic sections, and estimated a total volume of 18 km^3 DRE. The historical eruptions that formed the Islas Quemadas domes in the center of the lake in AD 1879–1880 were reported by Montessus de Ballore (1888) and later transcribed by Williams and Meyer-Abich (1955) and discussed by Golombek and Carr (1978). The three older tephra deposits TB2–TB4 associated with the Ilopango caldera were identified and briefly described in recent geologic and volcanologic studies done by the governments of El Salvador and Italy as a result of the 1986 San Salvador earthquake.

High-Precision $^{40}Ar/^{39}Ar$ age-dates of Quaternary Tephra

In 1991 two of us (F.M.C. and A.D.) made a transect of the Guatemalan Highlands from the Amatitlán caldera, south of Guatemala City, to north of the Atitlán caldera, collecting 1-kg samples from major ash-flow tuffs and fall deposits from type sections as described by Koch and McLean (1975) and subsequent authors. Whenever possible, large pumice fragments were collected to prevent sample contamination with free xenocrysts of older rocks admixed with tephra. Pumice fragments were gently crushed to liberate mineral phases, and a Frantz magnetic separator was used to separate feldspars from glass and mafic minerals of the medium grain-size fraction. We successfully dated five tephra units using the high-precision $^{40}Ar/^{39}Ar$ dating method (Figs. 3–6; Tables 1–3). Our initial goal was to date the majority of Quaternary tephra units, but the general absence of an appropriate high-K mineral phase – sanidine is exceedingly rare and hornblende and biotite are nearly always corroded and altered – precluded this. Stepwise heating experiments with apparently fresh biotite grains from the Los Chocoyos and T ash-

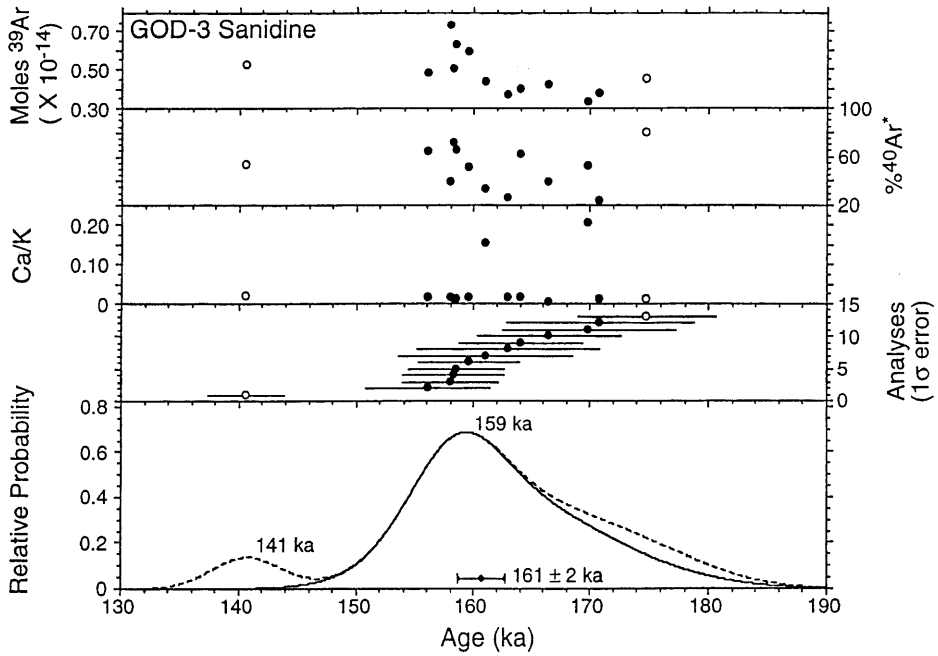

Fig. 3 Age-probability density diagram for sanidine from sample GOD-3 of the W air-fall tephra. The individual panels show, from top to bottom, (a) the number of moles of ^{39}Ar released from a sample, which is a function of grain size and potassium content, (b) the percent of radiogenic ^{40}Ar of the total ^{40}Ar argon released, (c) the Ca/K content of the grain, (d) an ordered display of individual analyses with 1-σ analytical errors, and (e) the age-probability density curve, calculated as the sum within narrow age intervals of 1-σ Gaussian error probabilities for each of the analyses (Deino and Potts 1992). *Open circles* represent outliers omitted from the weighted mean age (shown graphically as the *bar and tic symbol* beneath the main distribution). Solid age-probability curve excludes outliers; *dashed probability curve* includes all analyses. *Numbers* at the top of age-probability peaks are modal ages

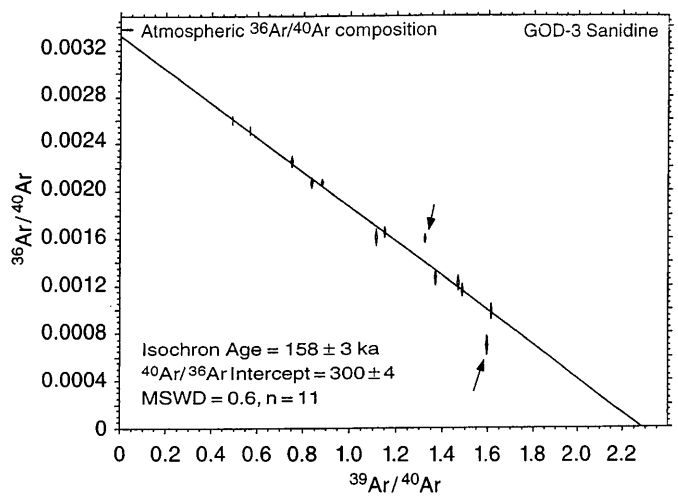

Fig. 4 A ^{36}Ar/^{40}Ar vs ^{39}Ar/^{40}Ar isochron for sample GOD-3 from the W air-fall unit. *Arrows* point to outliers excluded from analysis as discussed herein

flow deposits yielded poor results. Coatepeque tephras were sampled by CRP during 1996–1997 using similar techniques. Large, dense pumice fragments from a pyroclastic flow of the Bellavista unit and several large pumice clasts from fall deposits from the Arce and Congo units were collected.

The ^{40}Ar/^{39}Ar analyses were performed in two geochronology laboratories. Samples collected in the Guatemala Highlands from the Amatitlán to Atitlán caldera transect were analyzed at the Berkeley Geochronology Center (BGC) using the single-crystal total-fusion technique in the case of sanidine (tephra W; Table 1) and the furnace incremental-heating technique where only plagioclase feldspar was present (tephras I, T, X, and L; Table 2). Two sanidine and one hornblende separate from samples collected from the Coatepeque caldera (Bellavista, Arce, and Congo units) were analyzed at the New Mexico Geochronology Research Laboratory (Fig. 6; Table 3) using the furnace incremental-heating technique. Details of the techniques employed in the dating process are provided in the tables and in Deino and Potts (1990), Sharp et al. (1996), and McIntosh and Chamberlin (1994).

Sanidine from a tephra sample of the W fall collected near Godinez (GOD-3) was analyzed by the single-crystal laser-fusion technique (Table 1). The age-probability density spectrum of the 13 analyzed grains is given in Fig. 3. The distribution shows one clear outlier, younger in apparent age than the bulk of the distribution (the cause of this anomalous young apparent age remains unknown), and a slight tailing toward older ages for the remainder of the distribution. In the final calculations, we eliminated two outliers, taken as those analyses falling two standard deviations or greater from the mean (Fig. 3; Table 1). The weighted-mean age is little changed with or without these values, 161 ± 2 ka

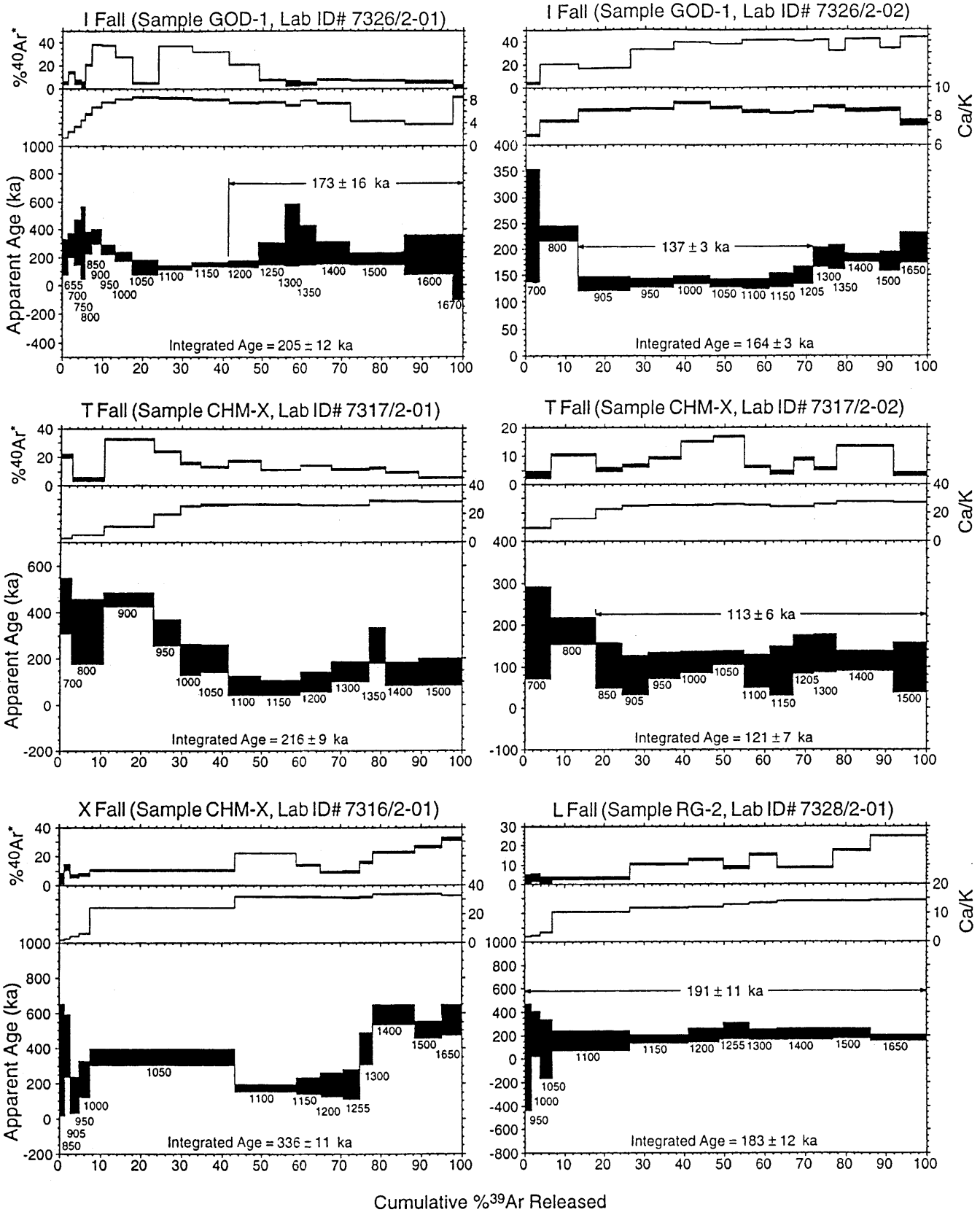

Fig. 5 Furnace-degassing, incremental-heating, apparent-age spectra from plagioclase experiments at Berkeley Geochronology Center. *Numbers* below apparent age bars are furnace temperatures (°C). Errors are stated in sigma

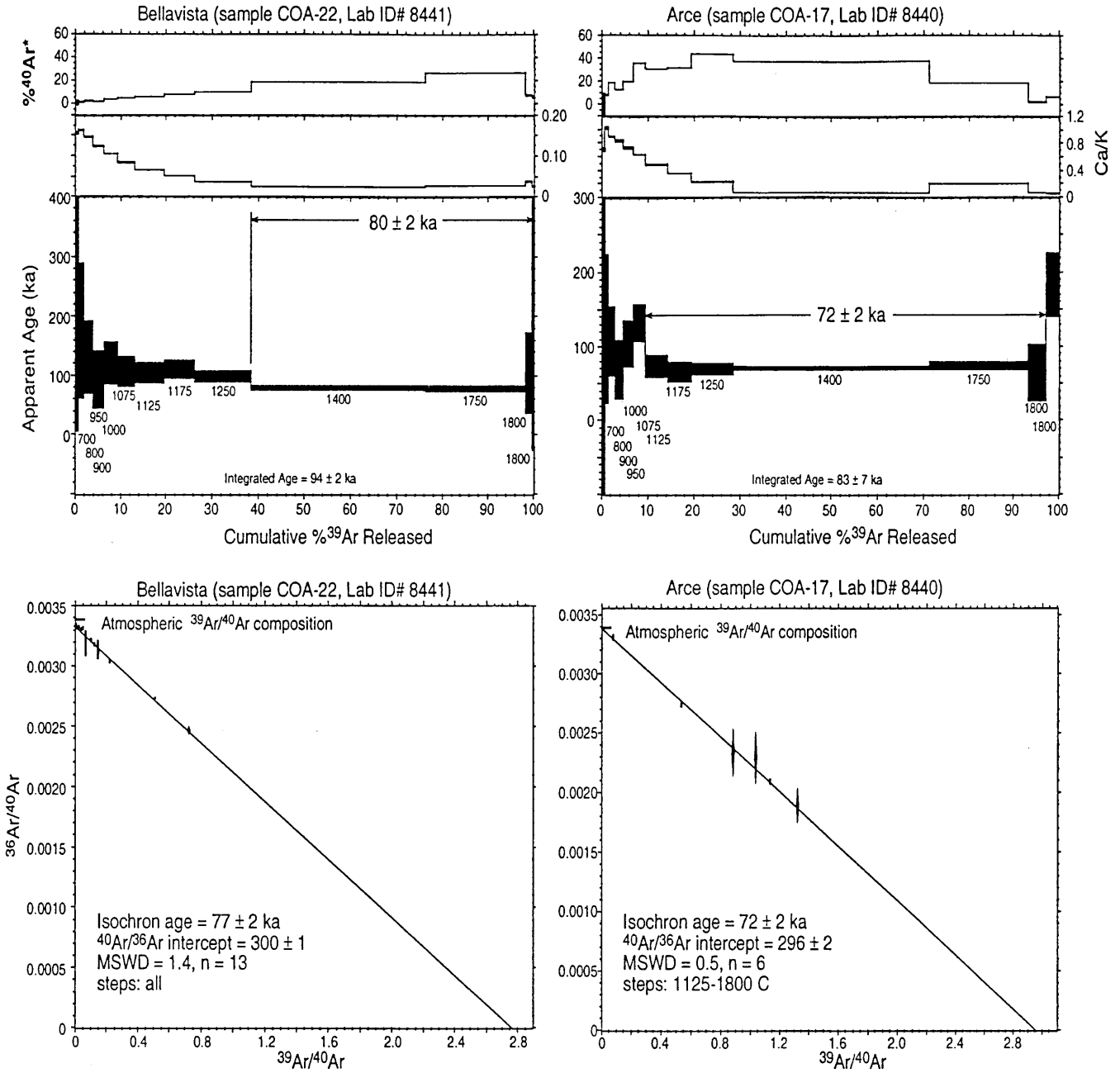

Fig. 6 Age spectra and isochrons for sanidine samples COA-22 (Bellavista pyroclastic flow) and COA-17 (Arce pyroclastic fall deposit). *Numbers* below the apparent age bars are furnace temperatures in (°C). Errors are stated in sigma. Below each spectra is the corresponding $^{36}Ar/^{40}Ar$ vs $^{39}Ar/^{40}Ar$ isochron

without outliers and 158 ± 3 overall. A $^{36}Ar/^{40}Ar$ vs $^{39}Ar/^{40}Ar$ isochron obtained from the data excluding outliers gives a trapped $^{40}Ar/^{36}Ar$ intercept of 300 ± 4 (statistically indistinguishable from the atmospheric value of 295.5), and an MSWD of 0.6, indicating acceptable statistics for the isochron fit and an age of 158 ± 3 ka, within error equivalent to the weighted-mean age (Fig. 4). The isochron age of 158 ± 3 ka is the best reference age for this sample. The concordance of the isochron and weighted mean ages, radiogenic argon yields typical of sanidine of this age, and the unimodal age distribution (excluding the young outlier) suggest that this is a geologically accurate age.

Sanidine is the preferred mineral phase in $^{40}Ar/^{39}Ar$ dating of young tephras, but it is absent from the older units sampled along the Amatitlán to Atitlán transect, so plagioclase was analyzed instead. Incremental heating of bulk samples was employed to examine the plagioclase mineral separates systematically, since individual plagioclase grains of this age do not yield enough ra-

Table 1 $^{40}Ar/^{39}Ar$ analytical data, Guatemala tephra W (air fall), sample GOD-3

Lab ID no.	Ca/K	$^{36}Ar/^{39}Ar$	$^{40}Ar^*/^{39}Ar$	% $^{40}Ar^*$	Age (ka) $\pm 1\,\sigma$
5929/2B-05	0.0144	0.00084	0.434	63.8	156 ± 5
5982/2-02	0.0146	0.00235	0.440	38.8	158 ± 4
5929/2B-08	0.0130	0.00061	0.440	71.0	158 ± 4
5929/2B-10	0.0100	0.00078	0.441	65.6	158 ± 4
5929/2B-01	0.0166	0.00144	0.444	51.1	160 ± 4
5929/2B-03	0.1536	0.00302	0.448	33.6	161 ± 7
5928/2-04	0.0139	0.00444	0.454	25.7	163 ± 8
5929/2B-09	0.0158	0.00093	0.457	62.4	164 ± 5
5929/2B-06	0.0026	0.00248	0.464	38.7	166 ± 6
5929/2B-04	0.2059	0.00147	0.473	52.5	170 ± 7
5928/2-01	0.0115	0.00531	0.475	23.3	171 ± 8
			Weighted average, σ error without error in J =		161 ± 2
			σ error with error in J =		± 2
Outliers					
5929/2B-02	0.0179	0.00118	0.391	53.0	141 ± 3
5929/2B-07	0.0114	0.00043	0.486	79.5	175 ± 5

Errors in age quoted for individual runs are 1-σ analytical uncertainty. Weighted averages are calculated using the inverse variance as the weighting factor (Taylor 1982), whereas errors in the weighted averages are 1-σ standard error of the mean (Samson and Alexander 1987). Ca/K is calculated from $^{37}Ar/^{39}Ar$ using a multiplier of 1.96. $^{40}Ar^*$ refers to radiogenic argon. $\lambda = 5.543 \times 10^{-10}$ y^{-1}. Samples were irradiated for 15 min in the hydraulic rabbit facility of the Omega West Reactor of the Los Alamos National Laboratory, using a Cd-lined sealed aluminum capsule. Sanidine from the Fish Canyon Tuff of Colorado was used as the monitor mineral, with a reference age of 27.84 Ma (Cebula et al. 1986, after Samson and Alexander 1987). Single sanidine grains were fused using an Nd-YAG laser under ultra-high vacuum and analyzed in a MAP-215-50 noble-gas mass spectrometer for five argon isotopes. $J = (1.992 \pm 0.01) \times 10^{-4}$. Isotopic interference corrections: $(^{36}Ar/^{37}Ar)_{Ca} = (2.58 \pm 0.06) \times 10^{-4}$, $(^{39}Ar/^{37}Ar)_{Ca} = (6.7 \pm 0.3) \times 10^{-4}$, $(^{40}Ar/^{39}Ar)_{K} = (8 \pm 7) \times 10^{-4}$

diogenic argon for accurate single-crystal analyses and argon distribution in plagioclase is often nonuniform. The results of these incremental-heating experiments are mixed in terms of inferred geologic reliability. Of the six experiments (two samples were analyzed in replicate), four yielded strictly defined plateaus (using the criterion of Fleck et al. 1977), which normally indicate a geologically reliable age. However, these samples in general exhibit "saddle-shaped" spectra, yielding older apparent ages at the beginning and ends of the heating sequence. Saddle-shaped spectra commonly suggest the presence of extraneous argon. When dating very young plagioclase with low K content, extraneous argon can seriously affect the reliability of a $^{40}Ar/^{39}Ar$ age.

Extraneous argon is apparently present, for example, in sample GOD-1 (Tephra "I" airfall). One of two replicate experiments (7326/202) clearly shows a saddle-shaped spectrum (i.e., older ages at the beginning and end of the sequence) (Fig. 5) but yields a plateau toward the center third at 137 ± 3 ka. Isochron analysis ($^{36}Ar/^{40}$ Ar vs $^{39}Ar/^{40}Ar$), which is often useful in detecting the presence of extraneous argon, in this case indicates a $^{39}Ar/^{40}Ar$ for the "trapped" argon composition of the sample of 294.0 ± 5.3 ka, within error of the expected atmospheric value of 295.5. The isochron intercept age of the plateau steps is 138 ± 5 ka. This apparent age is clearly far too old for the known stratigraphy, which indicates an age less than approximately 84 ka, the oxygen-isotope age of the stratigraphically older Los Chocoyos eruption. The second aliquot from this tuff yielded a flat spectrum with a plateau of 173 ± 16 ka (Fig. 5). The isochron gave slight indication of extraneous argon, yielding a trapped $^{40}Ar/^{36}Ar$ ratio of 300.9 ± 1.8, with an isocrhon age of 147 ± 12 ka. If, as we believe, the oxygen-isotope age of the Los Chocoyos eruption is accurate, it is apparent that extraneous argon in the "I" fall plagioclase has resulted in geologically inaccurate apparent ages.

Replicate resistance-furnace step-heating experiments on an air-fall tephra sample from the "T" eruption may be another example of extraneous argon. The incremental-release spectrum from the first aliquot showed a marked departure from the flat release expected of a well-behaved pristine volcanic material (Fig. 5), with too-old apparent ages (up to 450 ka) persisting through 40% of the total ^{39}Ar release, then reaching a shallow low apparent age of ~80 ka. The final 40% of the gas release also shows a climb toward older apparent ages, abeit less steep. These release characteristics (a crude saddle shape, with only a short middle "plateau") indicate complex internal argon systematics in the sample possibly attributable to extraneous argon. The second aliquot showed much less pronounced saddle-shaped behavior, with elevated ages in only the initial 20% of the release (Fig. 5). The remainder of the spectrum defined a plateau with an age of 113 ± 6 ka (Table 2). An isochron analysis of this portion of the spectrum gives an age of 119 ± 8 ka with a $(^{40}Ar/^{36}Ar)_{trapped}$ intercept of 293.2 ± 2.2, within error of atmosphere. The age of approximately 119 ka may be geologically accurate, but given the discrepant behavior of the spectra and the implications to be drawn

Table 2 $^{40}Ar/^{39}Ar$ analytical data, incremental-heating furnace analyses

Lab ID no.	C	Ca/K	$^{36}Ar/^{39}Ar$	$^{40}Ar^*/^{39}Ar$	^{39}Ar (mol × 10^{17})	% ^{39}Ar (of total)	% $^{40}Ar^*$	Age (ka 1σ)	
Sample GOD-1; I fall deposit; J = *5.034, 0.050*									
7326/2-01C	653	1.4	0.1432	2.233	23.1	1.4	5.0	203	63
7326/2-01D	702	2.5	0.0667	3.141	27.7	1.7	13.8	285	44
7326/2-01E	752	3.4	0.1976	3.414	24.5	1.5	5.5	310	82
7326/2-01F	802	4.5	0.3476	3.385	17.4	1.0	3.2	307	130
7326/2-01G	850	5.6	0.0453	3.374	28.2	1.7	20.4	306	39
7326/2-01H	900	6.8	0.0220	3.864	38.6	2.3	38.3	351	27
7326/2-01I	952	7.7	0.0168	2.788	58.8	3.5	37.4	253	17
7326/2-01J	1000	8.3	0.0219	2.294	68.2	4.1	27.1	208	16
7326/2-01K	1052	8.6	0.0978	1.410	108.5	6.5	4.7	128	27
7326/2-01L	1101	8.4	0.0088	1.358	138.4	8.3	37.5	123	7
7326/2-01M	1152	8.2	0.0125	1.617	150.2	9.0	32.4	147	8
7326/2-01N	1201	7.6	0.0226	1.691	128.8	7.8	21.0	154	12
7326/2-01O	1252	7.7	0.1036	2.497	110.0	6.6	7.6	227	40
7326/2-01P	1299	7.2	0.3060	4.012	64.7	3.9	4.3	364	112
7326/2-01Q	1349	8.0	0.2455	3.143	68.9	4.1	4.2	285	71
7326/2-01R	1399	7.4	0.1069	2.560	141.9	8.5	7.5	232	41
7326/2-01S	1501	4.4	0.0936	2.066	208.7	13.4	7.0	188	22
7326/2-01T	1600	3.8	0.1325	2.383	195.5	11.8	5.7	216	71
7326/2-01U	1671	8.6	0.4047	1.413	44.7	2.7	1.2	128	117
						Plateau age =		173	16
						Integrated age =		205	12
Sample GOD-1; I fall deposit; J = *5.034, 0.050*									
7326/1-02B	701	6.6	0.2303	2.674	2.7	3.5	3.8	243	54
7326/2-02C	799	7.7	0.0339	2.524	7.2	9.6	20.6	229	8
7326/2-02D[a]	903	8.4	0.0258	1.475	9.9	13.0	16.8	134	7
7326/2-02E[a]	952	8.5	0.0114	1.494	8.4	11.0	32.9	136	4
7326/2-02F[a]	1000	8.9	0.0092	1.550	6.8	9.0	39.6	141	4
7326/2-02G[a]	1052	8.6	0.0093	1.483	5.8	7.8	38.3	135	4
7326/2-02H[a]	1101	8.4	0.0082	1.466	5.2	6.8	41.3	133	5
7326/2-02I[a]	1151	8.2	0.0086	1.539	4.6	6.0	41.2	140	7
7326/2-02J[a]	1203	8.3	0.0095	1.646	3.7	4.8	40.1	149	8
7326/2-02K	1302	8.7	0.0109	2.024	2.9	3.8	41.3	184	9
7326/2-02L	1352	8.6	0.0156	2.019	3.1	4.1	32.1	183	12
7326/2-02M	1398	8.4	0.0105	2.003	6.6	8.7	42.0	182	4
7326/2-02N	1501	8.4	0.0138	1.941	3.7	5.0	34.2	176	9
7326/2-02O	1652	7.5	0.0107	2.277	7.0	6.9	44.2	207	15
						Plateau age =		137	3
						Integrated age =		164	3
Sample T-fall; J = *4.723, 0.050*									
7317/2-01A	700	2.8	0.0632	5.141	19.2	2.7	21.7	438	60
7317/2-01B	802	5.3	0.2848	3.650	56.1	8.0	4.2	311	69
7317/2-01C	902	11.3	0.0386	5.302	86.5	12.4	32.6	452	15
7317/2-01D	949	19.8	0.0410	3.764	45.8	6.5	24.9	321	27
7317/2-01E	1002	25.3	0.0435	2.398	35.6	5.0	16.8	204	34
7317/2-01F	1052	26.1	0.0555	2.507	49.5	7.0	13.9	214	29
7317/2-01G	1102	26.3	0.0189	1.036	58.1	8.2	18.6	88	21
7317/2-01H	1152	26.5	0.0270	0.958	71.1	10.0	12.1	82	17
7317/2-01I	1202	25.6	0.0266	1.218	55.1	7.8	15.1	104	22
7317/2-01J	1299	26.1	0.0457	1.800	67.4	9.5	12.5	153	22
7317/2-01K	1351	29.2	0.0770	3.028	27.1	3.9	12.2	258	39
7317/2-01L	1399	28.6	0.0562	1.716	57.7	8.1	9.9	146	26
7317/2-01M	1501	28.4	0.1031	1.917	76.7	10.8	6.1	163	30
						Integrated age =		216	9
Sample T-fall; J = *4.723, 0.050*									
7317/1-02B	701	9.3	0.2199	2.102	1.8	6.4	3.1	179	55
7317/2-02C	801	16.0	0.0643	2.179	2.1	11.4	10.6	186	16
7317/2-02D[a]	849	22.4	0.0760	1.218	0.4	6.6	5.3	104	28
7317/2-02E[a]	903	25.1	0.0484	0.950	−0.8	6.7	6.6	81	24
7317/2-02F[a]	950	25.2	0.0426	1.223	2.9	8.0	9.5	104	16
7317/2-02G[a]	1002	25.4	0.0276	1.311	2.9	8.1	15.5	112	13
7317/2-02H[a]	1050	25.8	0.0268	1.440	2.6	7.6	17.2	123	8
7317/2-02I[a]	1100	25.4	0.0568	1.057	2.3	6.4	6.2	90	20
7317/2-02J[a]	1149	24.3	0.0858	1.058	2.2	5.9	4.1	90	29
7317/2-02K[a]	1203	24.5	0.0547	1.526	1.8	5.0	9.1	130	23

Table 2 (Continued)

Lab ID no.	C	Ca/K	$^{36}Ar/^{39}Ar$	$^{40}Ar^*/^{39}Ar$	^{39}Ar (mol $\times 10^{17}$)	% ^{39}Ar (of total)	% $^{40}Ar^*$	Age (ka 1σ)	
7317/2-02L[a]	1300	26.1	0.0918	1.550	2.1	5.6	5.6	132	23
7317/2-02M[a]	1400	27.4	0.0324	1.361	5.4	14.0	13.7	116	12
7317/2-02N[a]	1501	27.3	0.1060	1.152	3.3	8.3	3.6	98	30
						Plateau age =		113	6
						Integrated age =		121	7
Sample CHM-X–X fall; J = *4.679, 0.050*									
7316/1-01E	849	2.1	0.2539	3.934	0.4	1.2	5.0	332	157
7316/2-01F	903	2.8	0.1205	4.869	0.5	1.6	12,1	411	88
7316/2-01G	950	4.5	0.0776	1.581	0.7	2.2	6.5	133	51
7316/2-01H	1002	6.8	0.1134	2.632	0.9	2.6	7.3	222	51
7316/2-01I	1052	24.6	0.1247	4.102	12.5	35.8	10.2	346	23
7316/2-01J	1101	32.3	0.0281	2.078	5.4	15.5	22.7	175	11
7316/2-01K	1151	32.0	0.0509	2.230	2.1	6.1	13.8	188	23
7316/2-01L	1201	31.8	0.0801	2.305	2.0	5.7	9.2	195	34
7316/2-01M	1252	31.5	0.0800	2.345	1.5	4.2	9.4	198	42
7316/2-01N	1302	32.1	0.0880	4.701	1.2	3.4	15.8	397	46
7316/2-01O	1402	34.1	0.0833	6.985	3.5	10.1	22.9	590	28
7316/2-01P	1501	34.0	0.0594	5.966	2.4	6.7	26.7	504	25
7316/2-01Q	1652	32.9	0.0514	6.636	2.2	5.0	32.1	560	44
						Integrated age =		336	11
Sample RG-2–L flow; J = *5.054, 0.050*									
7328/1-01G[a]	952	1.9	0.5151	0.116	0.5	1.5	0.1	11	225
7328/2-01H[a]	1000	2.3	0.2325	2.331	0.7	2.2	3.3	212	95
7328/2-01I[a]	1052	3.2	0.3495	0.901	1.0	3.1	0.9	82	125
7328/2-01J[a]	1100	10.3	0.1790	1.688	6.4	19.5	3.1	154	41
7328/2-01K[a]	1149	11.8	0.0561	1.836	4.8	14.7	10.2	167	17
7328/2-01L[a]	1201	12.1	0.0529	2.190	2.8	8.5	12.6	200	30
7328/2-01M[a]	1252	13.0	0.0961	2.608	2.1	6.5	8.5	238	35
7328/2-01N[a]	1302	13.6	0.0442	2.277	2.2	6.8	15.4	208	24
7328/2-01O[a]	1400	14.1	0.0847	2.321	4.6	13.9	8.6	212	25
7328/2-01P[a]	1501	14.1	0.0394	2.409	3.1	9.2	17.8	220	20
7328/2-01Q[a]	1652	14.4	0.0216	1.983	5.7	14.0	25.4	181	12
						Plateau age =		191	11
						Integrated age =		183	12

Ca/K is calculated from $^{37}Ar/^{39}Ar$ using a multiplier of 1.96. $^{40}Ar^*$ refers to radiogenic argon. Samples were irradiated (or 10 min in the Cd-lined CLICIT facility in the core of the Oregon State University TRIGA reactor at a power level of 1 MW. The neutron fluence monitor is sanidine from the Fish Canyon Tuff of Colorado with a reference age of 27.84 Ma (Cebula et al. 1986, after Samson and Alexander 1987). Approximately 0.18 to 0.25 mg of plagioclase were incrementally heated in a resistance under ultra-high vacuum and analyzed in a MAP-215-50 noble-gas mass spectrometer for five argon isotopes. Isotopic interference corrections: $(^{36}Ar/^{37}Ar)_{Ca} = 2.72 \times 10^{-4}$, 1×10^{-6}; $(^{39}Ar/^{37}Ar)_{Ca} = 7.11 \times 10^{-4}$, 2×10^{-6}; $(^{40}Ar/^{39}Ar)_K = 7 \times 10^{-4}$, 3×10^{-4}. $\lambda = 5.543 \times 10^{-10}$ y^{-1}

[a] Steps included in plateau calculations

from sample GOD-1, it also may be too old; nevertheless, at the least it provides a potentially useful maximum age.

Sample CHM-X (Tephra "X" airfall) yielded an irregular plateau with a rough saddle shape (Fig. 5). The middle portion of the spectrum yields a low "plateau" of limited extent with an age of approximately 190 ka, but the subsequent steps are much older in age, approximately 400–600 ka. This sample is clearly unreliable and may be considered another example of the presence of extraneous argon. Note that the pseudo-plateau age of approximately 190 ka is stratigraphically too old compared with the sanidine age of 160 ka on the immediately underlying "W" airfall tephra.

The final incremental-release sample is from sample RG-2 (Tephra "L" ash-flow tuff; Fig. 5). This sample exhibits an ideal, flat spectrum with a plateau age of 191 ± 11 ka, an isochron age of 193 ± 10 ka, and a $(^{40}Ar/^{36}Ar)_{trapped}$ intercept of 295.0 ± 1.9, within error of atmosphere. There is no analytical reason to suspect this age, and it accords with the few known calibrated stratigraphic constraints. Provisionally this is taken as a geologically accurate result.

Sanidine (Bellavista pyroclastic flow and Arce fall deposit) and hornblende (Congo fall deposit) from the Coatepeque caldera were analyzed using the furnace incremental-heating technique, chosen because the small crystal size and young age precluded single-crystal laser-fusion methods. Hornblende from the Congo fall deposit gave a strongly disturbed age spectrum with a geologically unreasonable integrated age of 1.2 Ma (Table 3). In addition, the data do not form a linear array on an isochron diagram. Results from this sample probably reflect inhomogeneously distributed extra-

Table 3 $^{40}Ar/^{39}Ar$ analytical data, incremental-heating furnace analyses

Lab ID no.	°C	Ca/K	$^{36}Ar/^{39}Ar$	$^{40}Ar/^{39}Ar$	^{39}ArK (mol × 10^{-17})	% ^{39}Ar (of total)	% ^{40}Ar*	Age (ka ± 1σ)
COA-21-Congo; hornblende; J = *0.00012113 ± 0.10, discrimination = 1.00799 ± 0.00121*								
8416-01A	800	1.25	0.0515	16.27	23.5	0.7	6.8	242 ± 61
8416-01B	850	2.14	0.0931	30.20	11.0	1.1	9.2	608 ± 127
8416-01C	950	2.82	0.1216	42.31	17.2	1.6	15.3	1418 ± 133
8416-01D	1020	5.51	0.0842	27.41	25.4	2.4	10.0	599 ± 96
8416-01E	1080	9.33	0.0339	11.29	138.0	6.7	14.4	357 ± 21
8416-01F	1120	9.10	0.0200	7.474	527.4	23.1	25.6	420 ± 8
8416-01G	1160	8.26	0.0146	7.228	538.5	39.9	45.0	712 ± 7
8416-01H	1200	4.18	0.0077	7.324	353.7	51.0	71.1	1140 ± 7
8416-01I	1300	0.94	0.0060	9.129	883.3	78.5	81.0	1615 ± 5
8416-01J	1400	0.04	0.0040	9.208	611.6	97.6	87.1	1751 ± 5
8416-01K	1650	2.64	0.0513	20.98	78.3	100.0	28.3	1298 ± 72
					Integrated age =			1156 ± 12
COA-22-Bellavista; sanidine; J = *0.00011731 ± 0.10%, discrimination = 1.0126 ± 0.00085*								
8441-02A	700	0.16	0.4672	140.1	70.7	0.7	1.4	427 ± 210
8441-02B	800	0.16	0.1567	47.12	126.2	1.9	1.8	176 ± 57
8441-02C	900	0.15	0.0889	26.90	202.0	3.8	2.3	132 ± 31
8441-02D	950	0.12	0.0708	21.35	253.6	6.3	2.1	93 ± 24
8441-02E	1000	0.11	0.0498	15.29	310.9	9.3	3.8	122 ± 18
8441-02F	1075	0.08	0.0325	10.09	410.2	13.2	5.0	107 ± 13
8441-02G	1125	0.07	0.0269	8.452	684.0	19.8	5.9	106 ± 9
8441-02H	1175	0.05	0.0213	6.813	687.9	26.5	7.8	112 ± 8
8441-02I	1250	0.04	0.0140	4.601	1261.5	38.6	10.3	100 ± 5
8441-02J¥	1400	0.02	0.0054	1.969	3939.3	76.6	19.2	80 ± 2
8441-02K¥	1750	0.03	0.0034	1.379	2265.8	98.4	27.2	79 ± 2
8441-02L¥	1800	0.04	0.0216	6.880	125.7	99.6	7.2	105 ± 34
8441-02M	1800	0.03	0.0485	15.22	40.8	100.0	5.9	189 ± 107
					Integrated age =			94 ± 8
					Plateau age (steps J–L) =			80 ± 2
					Isochron age (all steps) =			77 ± 2
COA-17 Arce; sanidine; J = *0.00011724 ± 0.10%, discrimination = 1.0126 ± 0.00085*								
8440-02A	700	0.72	1.1953	357.1	6.7	0.6	1.1	838 ± 981
8440-02B	800	1.02	0.0206	6.645	7.4	1.4	8.9	125 ± 50
8440-02C	900	0.90	0.0075	2.688	14.9	2.8	18.9	108 ± 23
8440-02D	950	0.84	0.0076	2.554	18.2	4.5	12.9	70 ± 20
8440-02E	1000	0.74	0.0066	2.424	23.4	6.8	20.3	104 ± 16
8440-02F	1075	0.63	0.0038	1.727	29.1	9.6	36.3	132 ± 12
8440-02G¥	1125	0.49	0.0027	1.130	49.3	14.3	31.1	74 ± 7
8440-02H¥	1175	0.36	0.0023	0.9679	51.6	19.2	32.4	66 ± 7
8440-02I¥	1250	0.23	0.0015	0.7565	96.5	28.5	44.2	71 ± 4
8440-02J¥	1400	0.07	0.0018	0.8808	447.2	71.3	38.4	71 ± 1
8440-02K¥	1750	0.21	0.0051	1.857	228.5	93.1	18.9	74 ± 3
8440-02L¥	1800	0.06	0.0433	13.11	42.5	97.2	2.3	65 ± 19
8440-02M	1800	0.06	0.0388	12.32	29.2	100.0	7.0	183 ± 21
					Integrated age =			83 ± 12
					Plateau age (steps G–L) =			72 ± 2
					Isochron age (steps G–L) =			72 ± 2

'¥' indicates steps included in plateau calculations. Ca/K is calculated from $^{37}Ar/^{39}Ar$ using a multiplier of 1.96. ^{40}Ar* refers to radiogenic argon. Samples were irradiated for 30 min in the boron-shielded D3 facility in the core of the Texas A & M University reator facility. Neutron flux was monitored with Fish Canyon Tuff sanidine with a reference age of 28.84 Ma (Cebula et al. 1986, after Samson and Alexander 1987). Sanidine was incrementally heated in a resistance furnace and analyzed in a MAP 215-50 mass spectrometer. Isotopic interference corrections: $(^{39}Ar/^{37}Ar)Ca = 0.00070 \pm 0.00005$, $(^{36}Ar/^{37}Ar)Ca = 0.00026 \pm 0.00002$, $(^{40}Ar/^{39}Ar)K = 0.0002 \pm 0.0003$. Decay constants after Steiger and Jaeger (1977). Plateau age criteria after Fleck et al. 1977, i.e. three or more contiguous steps, indistinguishable at $\pm 2\,\sigma$, comprising at least 50% of the total ^{39}Ar released

neous argon and are excluded from further consideration.

Sanidine from the Arce pyroclastic fall deposit (Sample COA-17) yielded a nearly flat age spectrum with a plateau age of 72 ± 2 ka (Fig. 6; Table 3). Data from the plateau steps also form a linear array on an isochron diagram, giving an isochron age of 72 ± 2 ka, a $^{40}Ar/^{36}Ar$ intercept of 296 ± 2, and an MSWD value of 0.5 (Fig. 6). An isochron plot of data from all heating steps gives an isochron age of 70 ± 2 ka, a $^{40}Ar/^{36}Ar$ intercept of 300 ± 2, and an unacceptably high MSWD value of 4.4. Given the high MSWD of this isochron and the small signal size of data from lower temperature heating steps, the isochron age of the plateau steps

Table 4 Ages and volumes of mid- to late-Quaternary pyroclastic events of Guatemala and western El Salvador. Italicized ages are new, documented in this paper

	Volume (km^3)	Age (ka)	Method
Atitlán			
I2-I5 falls[a,b]	7	>40	Stratigraphy
H fall and Los Chocoyos pf[c]	270–280	84 ± 0.5	Oxygen-isotope stratigraphy
W fall and pf	5–10	*158 ± 3 ka*[j]	$^{40}Ar/^{39}Ar$ single-crystal fusion
Amatitlán			
J fall[d]	0.2	<23	Stratigraphy
E fall[e]	2.5	>40	^{14}C
T fall and pf	>17	*119 ± 8*[k]	$^{40}Ar/^{39}Ar$
Z1–Z5 falls[e]	<0.1	>127; <182	Stratigraphy
L fall and pf	>18	*191 ± 11*[l]	$^{40}Ar/^{39}Ar$
Ayarza			
Piños Altos fall and flow[f]	2	23 ± 1	^{14}C
Mixta fall and flow[f]	<1	27 ± 2	^{14}C
Coatepeque			
Congo fall and pf[g]	6	*56.9 + 2.8/−2.1*[m]	High-sensitivity ^{14}C
Arce fall and pf[g]	17	70 ± 2	$K/^{40}Ar$
		72 ± 3[n]	$^{40}Ar/^{39}Ar$
Bellavista pf[g]	0.4	*77 ± 2*[o]	$^{40}Ar/^{39}Ar$
Ilopango			
TBJ fall and pf[h]	15–20	AD 260 ± 114	^{14}C
TB2–TB4 falls[i]	?	<40	Stratigraphy

[a] I fall is older than E fall (Koch and MacLean 1975)
[b] An $^{40}Ar/^{39}Ar$ of 138 ± 3 ka reported in this paper is rejected given stratigraphic constraint
[c] Drexler et al. (1980); Ledbetter (1985)
[d] J ash falls postdate the 23 ka Piños Altos deposit of Ayarza caldera (Koch and Mclean 1975; Peterson and Rose 1985)
[e] Wunderman and Rose 1984; McLean 1970
[f] Peterson and Rose (1985)
[g] Pullinger (1998)
[h] Hart and Steen-McIntyre (1983)
[i] CEL (1992a)
[j] GOD-1; Fig. 4, Table 1
[k] T-fall; Table 2, also see text
[l] RG-2, Table 2
[m] A-10094; see text
[n] COA-17; Table 3
[o] COA-22; Table 3

of 72 ± 2 ka (identical to the plateau age) is considered to be the most accurate determination of the eruption age of the Arce pyroclastic fall deposit.

Sanidine from the Bellavista pyroclastic flow (sample COA-22) yielded a gently falling age spectrum (Fig. 6; Table 3). Three of the higher-temperature heating steps meet plateau criteria, yielding a plateau age of 80 ± 2 ka. However, data from all of the heating steps form a well-defined isochron (Fig. 6) with an isochron age of 77 ± 2 ka, an acceptable MSWD of 1.4, and a $^{40}Ar/^{36}Ar$ intercept of 300 ± 1, suggesting a small amount of homogeneously distributed extraneous ^{40}Ar. This isochron age of 77 ± 2 ka is considered to be the most accurate determination of the eruption age of the Bellavista pyroclastic flow. The Arce age supports the earlier age reported by CEL (see above), and the age of the underlying Bellavista is stratigraphically consistent and only a few thousand years earlier. Unfortunately, there was no sanidine in the Congo samples, so dating was not possible. Because ^{14}C samples analyzed before have yielded >40 ka, we knew that the Congo eruption was between 70 and 40 ka (but see below).

In conclusion, sanidine found in the W and Arce fall deposits, and in the Bellavista pyroclastic flow, yield accurate, reliable ages of 158 ± 3 ka, 72 ± 2 ka, and 77 ± 2 ka, respectively. Step-heating experiments on plagioclase, however, apparently were influenced by the presence of extraneous argon in most of the aliquots. Some of these spectra nevertheless yield useful maximum ages and may prove to have provided geologically accurate ages as well (such samples as RG-2 and the T-fall tephra).

New high-sensitivity ^{14}C date

After the argon results led to unclear results, a single sample of carbon collected from the Congo pyroclastic flow at kilometer 59 on the PanAmerican Highway between Congo and Santa Ana was submitted to the University of Arizona radiocarbon lab for high-sensitivity dating by A. Long. The results (Arizona lab sample A-10094), corrected for ^{13}C, gave an age of 56.9 + 2.8/–2.1 ka.

The high-sensitivity date was performed as described by A. Long (pers. commun.): "The benzene synthesis system was flushed three times (Cal 274, Cal 275, Cal 276 in order of processing) prior to processing the unknown sample. We measured the ^{14}C content of Cal 274 and Cal 276 (Cal 275 was lost). Normally, we expect to see steady or decreasing 14 C in the sequence of flush samples, and we use the lowest measurement as a background for the calculation on the unknown. In this case, Cal 276 gave a result just measurably higher than Cal 274. We consider Cal 274 to be the more reli-

able indicator of background; Cal 276 might have become contaminated during catalyst stripping or loading in the counting vial. We therefore have two possible cases: (a) an age calculated with respect to Cal 274 (which is the result we favor, and is given above); and (b) an age calculated with respect to Cal 276, which is >55.4 ka, with an apparent age of 66.4 ka. In case 1, the result for A_{sn}/A_{on} (the activity ratio for sample to standard, after corrections) was 0.00084 ± 0.00025 (mean $\pm$ s) for the unknown. Since the mean is greater than $0+2\sigma$, a finite age can be given, and there is a 95% probability that the age lies in the range $0 \pm 2\sigma$. In case two, A_{sn}/A_{on} is 0.00026 ± 0.00025, and the mean is barely greater than $0+\sigma$. In such cases, there is a 95% probability that the age is greater than mean-2σ (55.4 ka)".

Discussion

Timing of volcanism at Atitlán caldera

Eruption of the W ash flow and ash-fall units at ca. 161 ± 2 ka marked the onset of the most recent episode of caldera-forming activity at Atitlán caldera (Table 4). The composite volume of the W fall and pyroclastic flow is 5–10 km^3 (Rose et al. 1987); however, exposures are obscured by younger deposits, and the volume could be larger than this estimate. Caldera formation at Atitlán culminated with the ca. 84-ka catastrophic eruption that produced the 270–280 km^3 Los Chocoyos Ash (Rose et al. 1979, 1981). The I2–I5 fall deposits overlie the C fall and mark the most recent silicic eruptions of the Atitlán caldera system. The perimeter of the Atitlán cauldron is home to three late-Quaternary to Holocene composite volcanoes: Atitlán, Toliman, and San Pedro. The volume of the I-fall deposits is approximately 7 km^3 (Rose et al. 1987). Our attempts to date these units yielded a geologically unreasonable isochron age of 138 ± 3 ka, whereas the ages of deposits as constrained by other stratigraphic data are between 40 and 119 ka. The difference in ages between the W fall and the H fall indicates recurrence of the order of 80,000 years at Atitlán. This is similar to recurrence rates for large-volume eruptions at Amatitlán caldera and suggests that length of repose and volume of the subsequent eruption at the two calderas are controlled by a common process (e.g., magma chamber recharge). The paucity of data at Atitlán warns against over-interpretation; nevertheless, this age analysis suggests that the Atitlán caldera could erupt again in the next several thousand years.

Timing of episodic pyroclastic activity at Amatitlán caldera

We report three new, geologically reasonable ages of the T-, W-, and L fall in Table 4 that help to constrain the activity at Amatitlán. The $^{40}Ar/^{39}Ar$ isochron age of 191 ± 11 ka reported here for the L flow is markedly younger than some previously reported ages (Ledbetter 1985) and consistent with a fission track age reported by Wunderman and Rose (1984; 300 ± 140 ka). It indicates that volcanism of the present generation of silicic calderas is confined to the past 200 ka. Importantly, the Amatitlán caldera formed when the L pyroclastic flow deposit, a single cooling unit comprising two discrete pyroclastic flows, erupted. The thickness of the L pyroclastic flow is at least 50 m, as measured in barrancos of the Guatemala City graben (Koch and McLean 1975); the 2-m-thick isopach of the underlying L fall extends at least 45 km north of Amatitlán (Wunderman and Rose 1984).

Caldera formation at Amatitlán was followed by repose punctuated by eruption of the small-volume, areally limited, Z1–Z5 ash-fall deposits (McLean 1970). The age of the Z-series ash-fall deposits is unknown but constrained between 158 ± 3 and $\leq 119 \pm 8$ ka by the stratigraphic position of Z between the W and T tephra.

The eruption of the T-fall and pyroclastic flows at $\leq 119 \pm 8$ ka marks the second major eruptive cycle at the Amatitlán caldera. This maximum age is consistent with a fission track age (240 ± 170 ka) reported by Wunderman and Rose (1984). The T ash flow moved more than 40 km north and northwest of the caldera, and valley-fill deposits exposed in barrancos in the Guatemala City graben are >100 m thick (Wunderman and Rose 1984). In addition, Ledbetter (1985) tentatively correlated the T fall with tephra recovered from DSDP core from the Pacific Ocean floor as far south as 6° S latitude. An oxygen-isotope age of 270 ka for ash from these cores, however, is inconsistent with the $^{40}Ar/^{39}Ar$ ages reported here, especially the sanidine age of 158 ± 3 on the W tephra, and suggests that (a) the correlation is invalid, or (b) problems exist with the oxygen isotope stratigraphy. The $^{40}Ar/^{39}Ar$ ages reported here for the L- and T falls show that repose between the major ash-flow eruptions at Amatitlán is at least 70 ka.

The eruption of the E fall deposits was the next major pyroclastic eruption of the Amatitlán caldera. Emplacement ages for these units are bracketed by the older Los Chocoyos deposit (84 ± 0.5 ka) and the younger Piños Altos fall deposit (23 ± 1 ka) of Ayarza caldera (Peterson and Rose 1985). In addition, McLean (1970) reported a ^{14}C age of >40 ka for the E fall. The youngest Amatitlán fall deposits, the J1, J2, and J3, overlie the ca. 23-ka Pinos Altos fall (Wunderman and Rose 1984), indicating that the caldera was active after 23 ka. Exogenous rhyolitic domes cropping out in the central and southwestern part of the caldera are broadly coeval with the E-fall deposit, suggesting a genetic relationship. The presence of active fumaroles and hot springs, and telltale geophysical and geologic evidence (e.g., the presence of the active basaltic Pacaya volcano) in the Amatitlán cauldron, led Wunderman and Rose (1984) to conclude that the caldera is still active. The $^{40}Ar/^{39}Ar$ isochron ages are consistent with an epi-

sodic volcanic system, with resurgence following large-volume ignimbrite eruption, involving 15–20 km^3 of tephra, occurring at intervals of ≥ 72 ka, based on the ages of the L- and T units. Interim periods are punctuated by infrequent small-volume pyroclastic events involving ~ 1 km^3 of fall accompanied by growth of rhyolitic domes. The timing of small-volume events is poorly constrained but has a recurrence rate of 20–30 ka. The last episode of pyroclastic activity occurred sometime shortly after 23 ka (Wunderman and Rose 1984); thus, it is possible that the Amatitlán silicic system is converging on a new episode of volcanic activity.

Volcanism at Coatepeque caldera

Silicic activity at Coatepeque Volcano began with the Bellavista eruption at 77 ± 2 ka (Table 4). The small volume Bellavista event was apparently triggered by basaltic intrusion into an evolved silicic magma body and had plinian and dome-building phases (Pullinger 1998). The voluminous Arce event occurred only a few thousand years later (72 ± 3 ka) and was likely the event in which the caldera formed. The age of the subsequent, slightly more mafic, Congo event ($56.9 + 2.8/-2.1$ ka) is 15,000 years younger. Activity of the Coatepeque caldera shows a pattern of spatial migration with time and has been marked by activity of mafic cones and domes since the Congo eruption (Pullinger 1998).

Stratigraphic intercalations

Besides providing information about the timing of activity at calderas, the new results allow constraints to be placed on the ages of several other important deposits in northern Central America, because of the stratigraphic relationships that are known based on the widespread occurrence of caldera deposits (Fig. 2):

1. The climatic eruptions of Siete Orejas can be constrained by their stratigraphic position between the W and H Atitlán deposits in the Totonicapán area (Rose et al. 1987, Fig. 11) at <158, >84 ka.
2. The dates of the deposits of the Barahona caldera (X, Y, and S deposits of MacLean (1970) are constrained by stratigraphy in the area near Antigua Guatemala, where these deposits overlie W and underlie T. This means that their ages are <158, $>\sim 119$ ka.
3. The Ilopango tephras TB2–TB4 can be constrained between <40 ka, $>$AD 260, based on their stratigraphic position overlying the youngest Coatepeque deposit and underlying TBJ.

Risk of eruptions from calderas in northern Central America

The risk of living with calderas should be compared with risks from other natural hazards associated with convergent plates: volcanic front volcanoes and tectonic earthquakes. Calderas are located near the economic hearts of both El Salvador and Guatemala; Guatemala City is on the north side and on an outflow sheet of Amatitlan, and San Salvador is on the west side and on an outflow sheet of Ilopango. They also are the scenic highlights of both countries and the site of major tourism development (Atitlán and Coatepeque). Because of their locations, near population, and their high-energy activity, caldera eruptions produce severely destructive hazards, especially when major pyroclastic flows are erupted. Caldera eruptions are less frequent (10^3–10^5 years) than eruptions from volcanic front volcanoes (every 1–10^3 years) or destructive tectonic earthquakes (ca. every 10^2–10^3 years). The vulnerability resulting from volcanic front volcanoes ranges from very low to moderately high, and vulnerability from earthquakes ranges from low to very high. But vulnerability from caldera activity ranges from moderate to extreme. Many of the eruptions in the geologic record would devastate most of the infrastucture of either Guatemala or El Salvador; thus, these volcanoes cannot be ignored despite their low probability of eruption.

Conclusion

New $^{40}Ar/^{39}Ar$ ages for five major units help to give a clearer picture of the timing of activity from the Quaternary silicic volcanoes north of the volcanic front in Guatemala and El Salvador. All five of the major Quaternary calderas of northern Central America have erupted several times in the past 200 ka. These centers have repose intervals from 10^3 to 10^5 years, and all should be considered potentially likely to erupt again.

The intercalation of fall deposits that are constrained by regional stratigraphic relationships has established a regional web of age information that should be widely useful to date Quaternary events.

Acknowledgements Financial support for this work came from the U.S. National Science Foundation, through grants EAR 9017821, INT 8915827, INT 9314794, and INT 9613647, and from the USGS through the VCAT/VDAP program. We acknowledge field help in Guatemala from J. Diehl, O. Matías, E. Sanchez, R. Morales, and N. Srimal. In El Salvador our colleagues at CEL (J. Rodriguez, R. Jacobo, L. Barrios, and S. Handal allowed us to use unpublished reports and provided vehicular support and office space. T. Soriano and R. Linares from the University of El Salvador participated in field work. A. Merla and V. Arno of Geothermica Italiana provided data on Coatepeque. S. Kelley and an anonymous reviewer helped improve the manuscript.

References

Cande SC, Kent DV (1995) Revised calibration of the geomagnetic polarity timescale for the Late Cretaceous and Cenozoic. J Geophys Res 100:6093–6095

Carr MJ, Stoiber RE (1990) Volcanism. In: Dengo G, Case JE (eds) The geology of North America: the Caribbean Region. Geol Soc Am Bull H: 375–391

Carr MJ, Rose WI, Stoiber RE (1981) Volcanism in Central America. In: Thorpe RS (ed) Orogenic Andesites and Related Rocks. J Wiley, NY, pp 146–166

Cebula GT, Kunk MJ, Mehnert HH, Naeser CW, Obradovich JD, Sutter JF (1986) The Fish Canyon Tuff, a potential standard for the ^{40}Ar–^{39}Ar and fission-track methods (abstract) Terra Cogn 6 (2): 139–140

CEL (Comision Ejecutiva Hidroelectrica del Rio Lempa) (1992a) Desarrollo de los Recursos Geotermicos del Area Centro-Occidental de El Salvador. Prefactibilidad Geotermica del Area de Coatepeque. Reconocimiento Geotermico. Informe Final. Internal report

CEL (Comision Ejecutiva Hidroelectrica del Rio Lempa) (1992b) Informe final del estudio geovulcanologico del campo geotermico de Ahuachapán. Contrato CEL-1771. Instituto de Investigaciones Electricas. Internal report

Conway FM, Diehl JF, Rose WI, Matias O (1994) Age and magma flux of Santa María Volcano, Guatemala: correlation of paleomagnetic waveforms with the 28,000 to 25,000 yr B. P. Mono Lake Excursion. J Geol 102:11–24

Deino A, Potts R (1990) Single-crystal $^{40}Ar/^{39}Ar$ dating of the Olorgesailie Formation, southern Kenya Rift. J Geophys Res 95:8453–8470

Deino A, Potts R (1992) Age-probability spectra for examination of single-crystal $^{40}Ar/^{39}Ar$ dating results: examples from Olorgesailie, southern Kenya Rift. Quaternary Int 7 (8): 81–89

Donnelly TW, Horne GS, Finch RC, Lopez-Ramos E (1990) Northern Central America: the Maya and Chortis blacks. In: Dengo G, Case JE (eds) The geology of North America: the Caribbean region, pp :37–76

Drexler JW (1979) Geochemical correlations of Pleistocene ryyolitic ashes in Guatemala with deep sea ashes of the Gulf of Mexico and equatorial Pacific. MS thesis, Michigan Technological University, 138 pp

Drexler JW, Rose WI, Sparks RSJ, Ledbetter MT (1980) The Los Chocoyos Ash, Guatemala: a major stratigraphic marker in Middle America and in three ocean basins. Quaternary Res 13:327–345

Eggers AA (1972) The geology and petrology of the Amatitlán Quadrangle, south central Guatemala. PhD dissertation, Dartmouth College, 221 pp

Fleck RJ, Sutter JF, Elliot DH (1977) Interpretation of discordant $^{40}Ar/^{39}Ar$ age-spectra of Mesozoic tholeiites from Antarctica. Geochim Cosmochim Acta 41:15–32

Golombek MP, Carr MJ (1978) Tidal triggering of seismic and volcanic phenomena during the 1879–1880 eruption of Islas Quemadas Volcano in El Salvador, Central America. JVGRDQ. J Volcanol Geotherm Res 3:299–307

Hahn GA, Rose WI, Meyers T (1979) Geochemical correlation of genetically related rhyolitic ash-flow and airfall ashes, central and western Guatemala and the Equatorial Pacific. In: Elston W, Chapin C (eds) Geol Soc Am Spec Pap 180:100–114

Halsor SP (1989) A comparative study of andesite at three stratovolcanoes, Lake Atitlán, Guatemala, PhD dissertation, Michigan Technological University, 323 pp

Halsor SP, Rose WI (1988) Common characteristics of active paired volcanoes in northern Central America. J Geophys Res 93:4467–4476

Halsor SP, Rose WI (1991) Mineralogical relations and magma mixing in calc-alkaline andesites from Lake Atitlán, Guatemala. Mineral Petrol 45:47–67

Hart WJE (1981) The Panchimalco tephra, El Salvador, Central America. MS thesis, Rutgers University, New Brunswick, New Jersey, 101 pp

Hart WJE (1983) Classic to Postclassic tephra layers exposed in archeological sites, eastern Zapotitan valley. In: Sheets PD (ed) The Zapotitán Valley of El Salvador: archeology and volcanism in Central America. Univ Texas Press, Austin

Hart WJE, Steen-McIntyre V (1983) Tierra Blanca Joven tephra from the A.D. 260 eruption of Ilopango. In: Sheets PD (ed) The Zapotitán Valley of El Salvador: archeology and volcanism in Central America. Univ of Texas Press, Austin, pp 14–43

Koch AJ, McLean H (1975) Pleistocene tephra and ash-flow deposits in the volcanic highlands of Guatemala. Geol Soc Am Bull 86:529–541

Ledbetter MT (1985) Tephrochronology of marine tephra adjacent to Central America. Geol Soc Am Bull 96:77–82

McIntosh WC, Chamberlin RM (1994) $^{40}Ar/^{39}Ar$ geochronology of Middle to Late Cenozoic ignimbrites, mafic lavas, and volcaniclastic rocks in the Quemado Region, New Mexico. New Mexico Geol Soc Guidebook, vol 45, pp 165–185

McLean H (1970) Stratigraphy, mineralogy and distribution of the Sumpango Group pumice deposits in the volcanic highlands of Guatemala. Ph D dissertation, University of Washington, 135 pp

Meyer J (1964) Stratigraphie der Bismskiese und -aschen des Coatepeque- vulkans im westlichen El Salvador (Mittelamerika). N Jahrb Geol Paläontol Abh 119:215–246

Meyer-Abich H (1956) Los Volcanes Activos do Guatemala y El Salvador, Anales Serv. Geol Nacl El Salvador Bd 3:49–62

Montessus de Ballore F (1888) Tremblements de terre et eruptions volcaniques au Cetre-Amerique, depuis la conquete espagnole jusqu'a nos jours. Soc Sci Natur Dijon, Saone-et-Loire, 293 pp

Newhall CG (1980) Geology of the Atitlán Calderas, Guatemala. Ph D dissertation, Dartmouth College, 364 pp

Newhall C (1987) Geology of the Lake Atitlán region, western Guatemala. J Volcanol Geotherm Res 33:23–55

Penfield GT, Rose WI, Halsor SP (1986) Geologic map of the Lake Atitlán volcanoes. Geol Soc Am Map and Chart Series, MC-55

Peterson PS, Rose WI (1985) Plinian eruptions of the Ayarza Calderas, Guatemala. J Volcanol Geotherm Res 25:289–307

Pullinger C (1998) Evolution of the Santa Ana volcanic complex, El Salvador. MS thesis, Michigan Technological University, 145 pp

Rose WI, Grant NK, Easter J (1979) Geochemistry of the Los Chocoyos Ash, Guatemala. In: Elston W, Chapin C (eds) Geol Soc Am Spec Pap 180:87–99

Rose WI, Drexler J, Penfield G, Larson PB (1980) Geochemistry of flank lavas of the three composite cones within the Atitlán Cauldron, Guatemala. Bull Volcanol 43:131–154

Rose WI, Hahn GA, Drexler JA, Love MA, Peterson PS, Wunderman RL (1981) Quaternary tephra of northern Central America. In: Sparks RSJ, Self S (eds) Tephra studies. Reidal, Holland, pp 193–212

Rose WI, Newhall CG, Bornhorst TJ, Self S (1987) Quaternary silicic pyroclastic deposits of Atitlán Caldera, Guatemala. J Volcanol Geotherm Res 33:57–80

Samson SD, Alexander EC Jr (1987) Calibration of the interlaboratory $^{40}Ar/^{39}Ar$ dating standard, MMhb-1. Chem Geol Isotherm Geosci 66:27–34

Sharp WD, Turrin BD, Renne PR, Lanphere MA (1996) The $^{40}Ar/^{39}Ar$ and K/Ar dating of lavas from the Hilo 1-km core hole, Hawaii Scientific Drilling Project. J Geophys Res 101:11607–11616

Steiger RH, Jager E (1977) Subcommission on geochronology: convention on the use of decay constants in geo- and cosmochronology. Earth Planet Sci Lett 36:359–362

Taylor JR (1982) An introduction to error analysis. University Science Books, Mill Valley, California

Wadge G (1984) Comparison of volcanic production rates and subduction rates in the Lesser Antilles and Central America. Geology 12:555–558

Williams H (1960) Volcanic history of the Guatemalan Highlands. Geol Sci 38:1–87

Williams H, Meyer-Abich H (1955) Volcanism in the southern part of El Salvador with particular reference to the collapse basins of Lakes Coatepeque and Ilopango. Geol Sci 32:1–64

Wunderman RL, Rose WI (1984) Amatitlán, an actively resurging caldera 10 km south of Guatemala City. J Geophys Res 89:8525–8539